

Stable kilohertz rate molecular beam laser ablation sources

Marc Smits and C. A. de Lange

Laboratory for Physical Chemistry, Nieuwe Achtergracht 127-129, 1018 WS Amsterdam, The Netherlands

Susanne Ullrich, T. Schultz,^{a)} M. Schmitt,^{b)} Jonathan G. Underwood,^{c)}
James P. Shaffer,^{d)} D. M. Rayner,^{e)} and Albert Stolow^{f)}

Steacie Institute for Molecular Sciences, National Research Council of Canada, Ottawa,
ON K1A 0R6, Canada

(Received 10 June 2003; accepted 7 August 2003)

We describe a stable kHz rate laser ablation/desorption supersonic molecular beam source for use in kHz rate laser experiments. With the development of modern lasers that typically operate at kHz rates, a need has arisen for stable molecular beam laser ablation/desorption sources for the study of involatile species. Many biomolecules of interest cannot be brought into the gas phase without thermal decomposition by simply heating the substrate and most (especially refractory) metals have melting and boiling points that are impossible to reach with conventional ovens. The source is based upon strong nonresonant interaction of a *dithering* laser focus with a rotating and translating solid rod, hydrodynamic transport of the ablated/desorbed material in helium or argon, and subsequent supersonic expansion. Further design details include flexible and easy adjustment of the source for rapid prototyping and optimization for kHz rate performance. Due to the high rate of sample removal, a major concern is clogging of the nozzle and laser input channel due to both material condensation and debris formation. In order to illustrate the range of applications, we demonstrate (1) the kHz laser ablation of a high temperature refractory metal (niobium) for use in studies of metal clusters; and (2) the kHz laser desorption and jet cooling of an involatile biomolecule (the DNA base guanine) for use in spectroscopic and dynamical studies. This kHz source design has been shown to be stable for over 12 continuous hours of operation ($>4 \times 10^7$ laser shots) and can be readily scaled to even higher repetition rates (>10 kHz). © 2003 American Institute of Physics. [DOI: 10.1063/1.1614879]

I. INTRODUCTION

The development of stable, commercially available kHz rate femtosecond laser systems has engendered many new classes of experimental investigation.¹ Such investigations in the gas phase are normally limited to gaseous or relatively volatile systems. The general application of kHz rate gas phase methods to involatile substances such as high temperature inorganic clusters or delicate biomolecules remains problematic. Simply heating the substrate to improve its vapor pressure is usually impossible for two reasons: first, many (especially transition) metals and inorganic solids have extremely high melting and boiling points; second, many bio-organic molecules thermally decompose upon heating. The use of laser ablation/desorption is one well-known technique that circumvents both these problems² and is the only way of producing refractory metal clusters. An important consideration in kHz rate femtosecond studies is the long-

term stability of the molecular beam source (e.g., flux, cluster distribution, internal and translational temperatures, etc.). As ablation sources are not inherently very stable, experiments based upon this technique generally require extensive signal averaging. In addition, many powerful experimental gas phase methods are based upon the small signal limit of particle counting. For example, femtosecond time-resolved photoelectron spectroscopies³⁻⁷ are generally restricted to small signals per laser shot in order to avoid higher optical nonlinearities due to the inherent high intensities of amplified fs pulses.⁸ The use of gas phase techniques such as photoelectron photoion coincidence (PEPICO) spectroscopy^{9,10} and coincidence-imaging spectroscopy [also known as angle-resolved PEPICO (ARPEPICO)]¹¹⁻¹⁴ require much less than one particle per laser shot and hence long signal averaging times. As it is often unfeasible to operate an ablation/desorption source over a period of many days, it is necessary to increase the laser repetition rate in order to reduce averaging times. Ideally, laser ablation/desorption sources should match the repetition rate of the femtosecond laser system. A second area where high repetition ablation sources are of interest are experiments that hinge upon large flux, such as those involving mass-selected deposition¹⁵ or direct linear absorption. If the ablation rate can be scaled without altering the concentration per pulse, significant saving of time can be achieved or, alternatively, less abundant species can be accumulated or studied.

^{a)}Present address: Max-Born-Institute for Nonlinear Optics and Ultrafast Spectroscopy, Berlin, Germany.

^{b)}Present address: Institut für Physikalische Chemie, Universität Würzburg, Würzburg, Germany.

^{c)}Present address: Department of Physics and Astronomy, The Open University, Milton Keynes, UK.

^{d)}Present address: Department of Physics and Astronomy, University of Oklahoma, Norman, OK.

^{e)}Electronic mail: david.rayner@nrc.ca

^{f)}Electronic mail: albert.stolow@nrc.ca

Laser ablation/desorption is governed by a series of complex processes, from the initial laser irradiation to the ejection of molecules and clusters, and depends sensitively on the laser wavelength (λ), the pulse duration (τ), the energy per pulse (E),^{16–18} the source design as it relates to the gas dynamics, as well as on optical, topological, and thermodynamic properties of the target material. Many experimental and theoretical reviews have summarized and categorized the different mechanisms involved,^{19–22} but sources are often developed on a trial and error approach. For the purpose of this discussion, we wish to distinguish between laser desorption and laser ablation. The former, of relevance to studies on involatile biomolecules, is predominantly in the regime of intermediate power densities and leads to the removal of neutral molecules from the surface. The latter, of interest to studies of inorganic and metallic clusters, requires high ablation laser power densities and, for high temperatures species, laser–plasma interaction.

A significant issue for kHz rate ablation sources is the clogging of the nozzle due to condensation and debris formation. The three most important processes for debris formation are recoil ejection, subsurface boiling, and exfoliation. Which of these is dominant depends on the target material and the laser characteristics. The first process, recoil ejection, is the result of the extremely high pressure in the nascent plasma. The melt on the surface of the plasma is squeezed to a droplet by the high pressure and produces particulates of less than a micron in size. The second process, subsurface boiling, is mainly a problem for metals with low melting points and high heat conductivity (e.g., aluminum). In this case, the time needed to heat the thermal diffusion layer is shorter than the time needed to evaporate the absorption surface. The explosive phase transition produces droplets similar to recoil ejection, although the ejection angles are different. The last process, exfoliation, is a result of extreme forces due to the highly energetic collisions of the ions from the plasma with the target bulk. Multiple melt–freeze cycles on the surface of the target roughen the surface and macroscopic particulates are formed. When these particulates break off by recoil forces, they may have dimensions of many microns and lead to source flow instabilities.

In the following, we present an overview of the design considerations for our highly versatile supersonic molecular beam source used in kHz rate femtosecond laser experiments. We illustrate its application in the areas of (i) atomic and cluster beams of a high temperature refractory metal (niobium); (ii) molecular and cluster beams of an involatile biomolecule which is considered difficult to produce using thermal methods (the DNA base guanine).

II. DESIGN

Modern kHz laser systems are available with pulse durations ranging from a few femtoseconds to hundreds of nanoseconds, and wavelengths ranging from the near UV to the infrared. For applications to laser ablation, the wavelength dependent absorption penetration depth and the target material dependent thermal diffusion rate have to be considered. For nanoseconds pulses, the thermal diffusion length in

a typical metal is orders of magnitude larger than the absorption depth. A large volume of molten material is typically formed and a strong reaction with any laser-induced plasma is expected. At the other extreme of femtosecond pulses, thermal diffusion can be neglected and the process is dominated by a highly nonlinear optical absorption processes. In the present study, three different laser systems with pulses ranging from 100 ps to 150 ns are successfully demonstrated as (i) an ablation source for the generation of transition metal clusters and as (ii) a desorption source of involatile biological molecules. Our most successful laser system for ablation is an arc lamp pumped Nd:YLF laser (Positive Light Merlin), producing pulses of >10 mJ/pulse in 150 ns at 527 nm. The second laser system, with only very moderate cluster production, is an NRC-design kHz diode-pumped grazing incidence Nd:YVO₄ slab laser with pulses of 1 mJ/pulse in 2 ns at 532 nm.²³ As an option this laser can be operated as a picosecond amplifier using a ps Nd:YAG oscillator (Lightwave Electronics 131) as a seed laser, shortening the 532 nm pulse to 100 ps. In this case, a very stable and clean source is achieved. Unfortunately densities of ablated species in the molecular beam are relatively low (approximately 10 times lower) and therefore we restrict the following discussion of kHz ablation sources to applications with the Nd:YLF laser. It is worth noting, however, that such diode-pumping technologies can be scaled to many tens of kHz repetition rate.

High throughput sources for applications in spectroscopy or thin film deposition have as a major concern the high gas load and, hence, high pumping speed requirements. Employing pulsed nozzle designs can present difficulties at kHz rates in terms of stability and reproducibility when heated to high temperatures. Moreover, little is gained in controlling throughput because of the limited duty cycle (often ~ 3). A continuous carrier gas flow has therefore been implemented in the present study.

As throughput, ease of use and adaptability are more important in our present experiments than is internal cooling, so we adopted a Campargue-type design²⁴ which operates at higher background pressure ($P_1 < 1$ Torr, with use of a standard booster pump), as opposed to the Fenn-type design^{25,26} which operates at a sufficiently low background pressure ($P_1 < 10^{-3}$ Torr, with use of large diffusion pumps) to avoid interference with the expansion. In Fig. 1 we show an overview of our triply differentially pumped vacuum chamber. The first or source region is pumped by an Edwards mechanical Roots blower (EH500A, 350 m³/h), allowing the source to operate in the Campargue-type configuration with background pressures of $< 10^{-1}$ Torr during operation. The molecular beam enters the second or differential region, via a 1 mm diam skimmer (Beam Dynamics), which is pumped by a single diffusion pump (Edwards Diffstak 250, 2000 l/s) to pressures of $< 10^{-4}$ Torr during operation. In this region, any residual ions formed during ablation are removed from the molecular beam by two deflection plates ($\Delta V_1 = \sim 250$ V). (It is in principle possible to operate in the Fenn-type configuration by closing off the Roots blower and opening a bypass, or by moving the source holder and skimmer into the second region.) The distance from the source to the point of interaction is kept as short as possible to maximize the beam

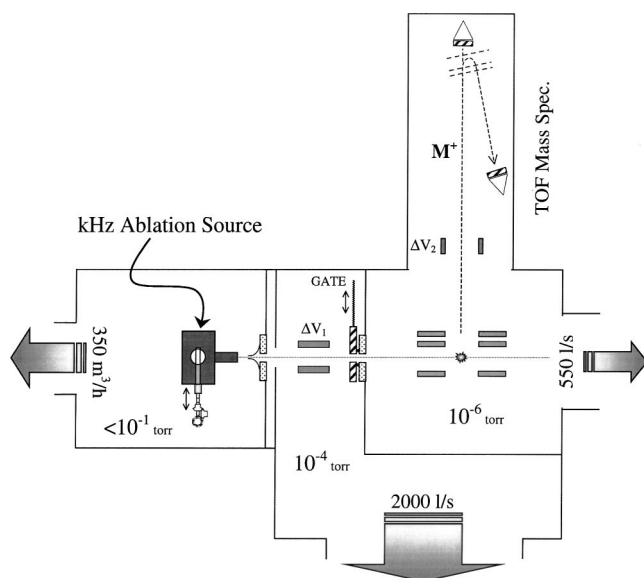


FIG. 1. The kHz ablation apparatus consists of three differentially pumped regions. The first or source region is pumped by a Roots blower ($350 \text{ m}^3/\text{h}$, $<10^{-1}$ Torr during operation). The molecular beam enters the second region, via a 1 mm skimmer, pumped by a single diffusion pump (2000 l/s , $<10^{-4}$ Torr during operation). Residual ions formed during ablation are removed from the molecular beam by two deflection plates ($\Delta V_1 = 250 \text{ V}$). The skimmed molecular beam passes through an aperture into the third or interaction region which is pumped by a turbomolecular pump (550 l/s) and contains the TOF mass spectrometer (both linear and reflectron). Another pair of deflection plates (ΔV_2) can be used to remove the initial molecular beam velocity, if required.

density at the laser focus. The third or interaction region is differentially pumped by a turbomolecular pump (Varian V550, 550 l/s) and houses a linear time-of-flight (TOF) mass spectrometer. This high vacuum region can be isolated from the other regions by an NRC-designed low profile gate valve.

In a kHz desorption/ablation source, the target material is removed at a sufficiently rapid rate that clogging of the nozzle and tooling of the substrate become serious problems. In our design, shown in Fig. 2, the target sample is a cylindrical rod of 6 mm diameter and up to 3 cm length. The source holder is a modified Smalley-type cluster source²⁷ and is designed for easy adjustment. The inset in Fig. 2 shows the nozzle block detail (top view). The nozzle itself is machined as a separate insert (shown in black) into this block and it functions as an optional growth channel. This allows for rapid prototyping and makes the source highly versatile. A variety of inserts with different diameters and lengths of growth channel, different materials of growth channel and nozzle, different diameters of the nozzle, and different diameters of the laser entrance aperture have been tested. Using a rotary motion feedthrough and an external stepper motor, the rod is simultaneously translated and rotated in helical fashion using a screw drive. Via bevel gears, the rotary motion of the drive leads to rotation of a perpendicular threaded shaft within an internally threaded block (shown in white). The sample rod mounts, via a hex key, into the top of this threaded shaft. The sample rod is constrained to move within another block (shown in gray) which also houses the nozzle insert. In this manner, a new sample spot can be provided to each ablation laser pulse in order to minimize the formation

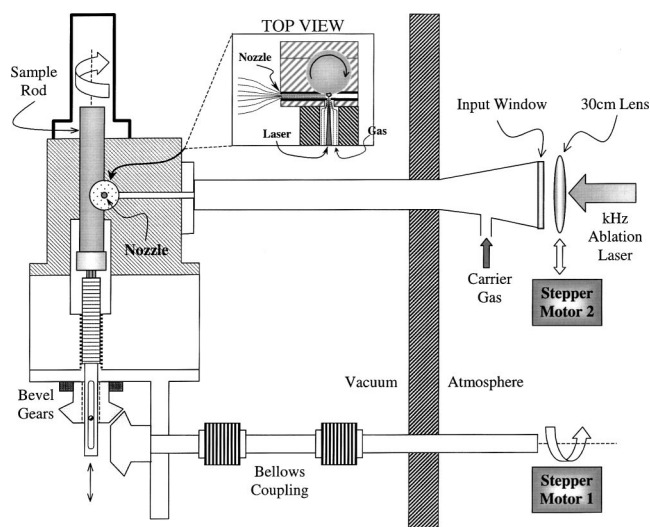


FIG. 2. Using a rotary motion feedthrough and an external stepper motor, the sample rod is simultaneously translated and rotated using a screw drive. The target is a cylindrical rod of 6 mm diameter and up to 3 cm in length. The source holder is a modified Smalley-type cluster source and allows easy adjustment. As shown in the inset, the nozzle is machined in a separate insert that functions as an optional growing channel. At the endpoints of the screw drive, the direction of the stepper motor is reversed and helical motion of the opposite sense occurs. The carrier gas is introduced along a long flow tube (also the laser input tube) and through a small aperture to the rotating sample, as shown in the (top view) inset. The length of the channel between the sample rod and the nozzle can be varied using different inserts (shown in black).

of deep pits and debris formation processes like exfoliation. At the endpoints of the screw drive, the direction of the stepper motor is reversed and helical motion of the opposite sense occurs. The carrier gas is introduced along a long flow tube (which also serves as the laser input tube) and through a small aperture to the rotating sample, as shown in the inset (top view) in Fig. 2. In this manner, debris ablated from the target surface does not reach the laser input window, which would otherwise become obscured over time. The distance from the laser input window to the sample rod is 25 cm. With a $f = 300 \text{ mm}$ lens, the ablation laser can be focused onto the target with minimum spot size of about $15 \mu\text{m}$. For most stable operation, however, the focus is pulled slightly backwards, yielding an estimated spot size of about $100 \mu\text{m}$. This provides upper limits for the maximum intensities of $\sim 10^9 \text{ W/cm}^2$ and maximum energy densities of $\sim 10^8 \text{ J/cm}^2$ for the 150 ns Nd:YLF laser. The use of separate inserts containing the nozzle and growth channel also allows easy exchange and cleaning. We have found that for stable long-term operation, both the nozzle and laser/carrier gas aperture diameters must be at least 2 mm. The length of the channel between the sample rod and the nozzle can be varied using different inserts. In some cases (e.g., metals), this length defines a clustering region that governs the cluster size distribution. Different materials for the growth channel and the nozzle have been tested, with standard glass being the most successful in our metallic cluster experiments. Depending on the characteristics of the growth channel, the time spent in the channel is up to several hundreds of microseconds and produces metallic (here niobium) clusters up to 40 atoms.

Accurate, stable control of the helium or argon (Air

Products, zero grade) buffer gas is achieved with mass flow controllers (MKS 1159B). Our pumps can support a continuous flow of up to 1400 sccm. With a growth tube 2 mm in diameter and approximately 1 cm in length, this corresponds to stagnation pressure of ~ 10 Torr at the throat of the nozzle. The buffer gas provides conditions for the cooling and clustering of the ablated/desorbed material by collisions in the source exit channel. In addition the large flow rate is important in keeping the channel and apertures in the source unclogged. With our design, flow rates below 800 sccm lead to clogging of the nozzle and laser aperture within 1 h of operation.

The motion of the rod should be sufficiently fast that a “fresh” surface spot can be presented to the ablation laser every millisecond (i.e., kHz rate), otherwise signal levels degrade quickly. Even this, however, is not sufficient for stable long-term operation. We have observed, due to the reproducibility of the helical track produced by the drive motion and the high rate of material removal, that a deep thread is cut into the rod. This leads to strong diminution and eventual loss of the signal. To avoid this, we *dithered* the up-down position of the laser focus, as shown in Fig. 2, by displacing the focusing lens slightly (with a ~ 0.1 Hz period, ~ 1 mm amplitude of travel) and, importantly, in an *asynchronous* manner, using a second stepper motor. With this approach, the pattern of laser spots on the rod surface does not produce regular helices. This simple modification allowed us to operate kHz rate ablation sources for over 12 continuous hours (i.e., $>4 \times 10^7$ laser shots). Upon inspection of the rod after such a long run, the rod diameter was significantly thinner but no thread pattern could be observed on the surface.

III. EXPERIMENT

The 50 cm time-of-flight mass spectrometer consists of a standard Wiley–McLaren and (optional) reflectron TOF mass spectrometer. Single ions are detected using Burle microchannel plate (MCP) detectors, fed directly into a pulse amplifier and discriminator (Phillips). Mass spectra are recorded using either a standalone multichannel scaler (Stanford Research SR430) or a PCI-based multichannel scaler (FastComtec P7888). In order to compensate for any potentially large lab-frame molecular beam velocities, deflection plates ($\Delta V_2 = 0 - 150$ V) can be used to remove the component of velocity perpendicular to the time-of-flight axis and thus straighten the ion trajectories. This can help to produce an essentially background free mass spectrum, depending on the mass of interest and the nature of ablation. In some cases, active background subtraction can be implemented in order to ensure the signal originates from laser ablation. This is simply achieved by alternating at 2000 shot intervals, with the ablation laser unblocked/blocked and the background signal subtracted.

The present National Research Council femtosecond laser system, depicted in Fig. 3, has been described in detail elsewhere.²⁸ Briefly, a fs Ti:Sapphire (Spectra-Physics Lok-to-Clok Tsunami) and a ps Nd:YAG (Lightwave Electronics 131) oscillator are individually locked, via phase-locked loops, to a stable 80 MHz external reference oscillator, thus

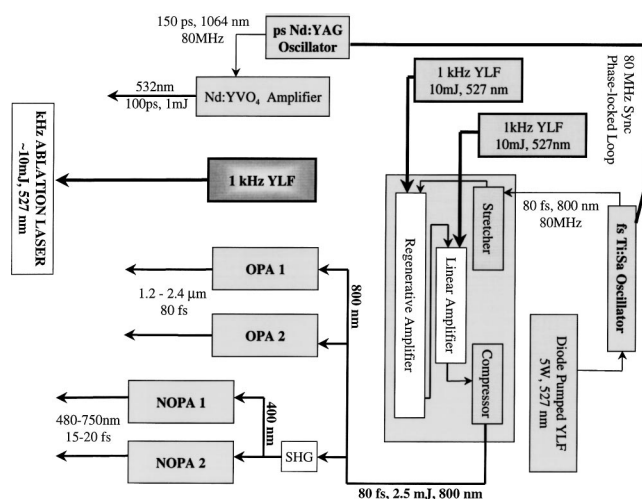


FIG. 3. A fs Ti:Sapphire (Spectra-Physics Lok-to-Clok Tsunami) and a ps Nd:YAG (Lightwave Electronics 131) oscillator are locked to a 80 MHz external reference oscillator. The Ti:Sapphire pulses are regeneratively amplified and subsequently passed through a two-pass linear Ti:Sapphire amplifier. Each Ti:Sapphire amplifier is pumped by a kHz Nd:YLF laser. After recompression, transform-limited 800 nm pulses of 80 fs and 2.7 mJ are obtained. The ps Nd:YAG pulses are amplified using an NRC-design kHz diode-pumped grazing incidence Nd:YVO₄ slab laser, which produces 1 mJ, 100 ps pulses at 532 nm. The amplified fs laser system pumps four optical parametric amplifiers (two Quantronix/LightConversion TOPAS, two Clark-MXR NOPA). An arc-lamp pumped kHz Nd:YLF laser (Positive Light Merlin), synchronized to the Ti:Sapphire lasers, is used for kHz rate ablation.

synchronizing the oscillators. The Ti:Sapphire pulses are regeneratively amplified (Positive Light Spitfire) using a diode-pumped Nd:YLF laser (Positive Light Evolution 30). These amplified pulses are subsequently passed through a two-pass linear Ti:Sapphire amplifier, pumped by another Nd:YLF laser (Positive Light Evolution 30). After recompression, transform-limited 800 nm pulses of 80 fs and 2.7 mJ are obtained. The ps Nd:YAG pulses are amplified using an NRC-design kHz diode-pumped grazing incidence Nd:YVO₄ slab laser,²³ which produces 1 mJ, 100 ps pulses at 532 nm. The arc lamp pumped Nd:YLF laser (Positive Light Merlin), with pulses of >10 mJ/pulse in 150 ns at 527 nm is synchronized with the fs laser system using a digital delay generator. The amplified fs laser system pumps four optical parametric amplifiers (two Quantronix/LightConversion TOPAS, two Clark-MXR NOPA). Laser pulse energies are monitored on a shot-to-shot basis using integrating spheres with photodiodes for kHz rate active data filtering and sorting.

IV. DEMONSTRATION AND APPLICATIONS OF kHz ABLATED BEAMS

A. Strong field ionization of transition metal clusters

As the first example of the use of kHz rate laser ablation sources, we discuss in the following aspects of our studies in the strong field ionization of metal clusters. Modern amplified femtosecond lasers can reach electric field strengths of $>10^9$ V/cm, exceeding those that bind matter. The study of strong field physics contributes to our understanding of strong field quantum control²⁹ and extreme nonlinear optics.³⁰ A technological application is in laser machining,

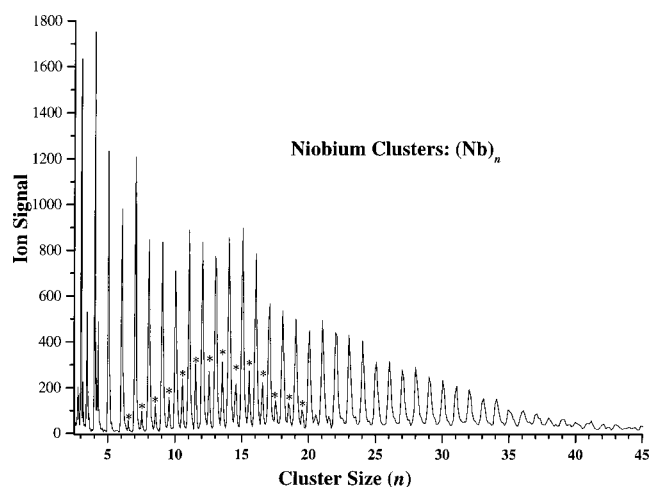


FIG. 4. Typical mass spectrum, recorded in 5 min, of kHz rate laser ablated niobium clusters, nonresonantly ionized at a laser intensity of $1 \times 10^{13} \text{ W/cm}^2$ ($\lambda = 0.8 \mu\text{m}$). With this particular growth channel, a broad cluster distribution is obtained with this method. The mass peaks marked by an asterisk are the doubly charged cluster species. This kHz source is stable for over 12 continuous hours of operation. For details, see the text.

where precise removal of material is possible by using laser intensities that exceed the damage threshold.³¹ Most current models of strong field interaction with matter are based upon the highly successful atomic quasistatic model.³² Recently, these quasistatic models have been shown to fail for certain classes of polyatomic molecules due to nonadiabatic multi-electron effects.³³ These studies showed that multi-electron effects exist (specifically, strong suppression of ionization) even in the long wavelength limit due to the effects of dynamic electron polarization. In this regard, the strong field ionization of metal clusters should provide an ideal test case for the role of dynamic polarizabilities. Using the saturation intensity method,³⁴ we have studied nonresonant ($\lambda = 0.8$ and $1.5 \mu\text{m}$) strong field ionization of size postselected metal clusters using kHz rate laser ablation as the molecular beam source.³⁵

In this study we chose niobium (Nb) as a model target metal. Nb is a typical transition metal with high melting and boiling points of 2477 and 4744 K,³⁶ respectively, and has the advantage of having only one natural isotope, thereby simplifying the mass spectrum. Using the laser ablation method described above, we were able to generate stable (>12 h) cluster beams at a 1 kHz rate. For studies of strong field ionization, we used both $\lambda = 0.8$ and $1.5 \mu\text{m}$ wavelengths. Typical pulse durations were ~ 80 fs. Absolute laser intensities ($\pm 30\%$) were determined using the saturation intensity method with xenon gas as a reference standard. For the $1.5 \mu\text{m}$ radiation, a maximum intensity of over $2 \times 10^{14} \text{ W/cm}^2$ at the focus was achievable. At $0.8 \mu\text{m}$, an order of magnitude higher intensity was achievable. A typical mass spectrum (recorded in 5 min) at an intensity of $1 \times 10^{13} \text{ W/cm}^2$ ($0.8 \mu\text{m}$) is shown in Fig. 4. Strong nonresonant field ionization of niobium clusters is clearly observed. A broad cluster distribution is obtained with this method. The mass peaks marked by an asterisk are the doubly charged cluster species. The stability of this source allows experiments of long duration (such as the saturation intensity

method which requires sampling over all laser intensities at each cluster mass) to be performed.

B. Pump–probe spectroscopy of gas phase biomolecules and their clusters

As the second demonstration of kHz rate ablation sources, we discuss in the following the study of involatile biomolecules in the gas phase. There is increasing interest in studies of biologically relevant molecules in the gas phase, triggered by the first applications of laser desorption/ablation techniques to involatile, organic molecules.^{37,38} The femtosecond pump–probe spectroscopic method, developed for the investigation of dynamical processes in photochemistry,³⁹ is now reaching into the area of photobiology.^{40,41} One approach to studying details of ultrafast excited state electronic relaxation processes such as internal conversion and intersystem crossing is femtosecond time-resolved photoelectron spectroscopy (TRPES).^{6,7,42} Due to its inherently low count rate, successful application of TRPES to involatile biological molecules demands a soft vaporization molecular beam source that is stable enough over an extended period of time to allow such spectra to be recorded.

In order to test our kHz laser ablation source for involatile biological molecules, we used the DNA base guanine as an example. As for many biomolecules, simple heating of guanine would lead to thermal decomposition before desorption.⁴³ Sample preparation for use in our ablation source involves pressing guanine powder (Sigma, 99% purity) into a 1/4 in. diam rod under 1–2 tons of pressure. Although only neat guanine was employed in this demonstration, rods consisting of biomolecules and matrices or mixtures of biomolecules can be readily prepared.

We demonstrate the successful application of our kHz laser ablation source to the generation of jet-cooled molecular beams of guanine. The kHz ablation laser (attenuated to 1 mJ/pulse) was focused ($f/30$) onto the rotating, translating neat guanine rod. The guanine vapor was expanded through a 1 mm diam orifice seeded in Ar at a flow rate of 1200 sccm. To probe the skimmed guanine molecular beam, we employed femtosecond laser (1+1) one-color resonant two-photon ionization of guanine at 277 nm ($15 \mu\text{J/pulse}$, 150 fs). We present an example of a mass spectrum of kHz laser ablated guanine in Fig. 5. [In order to demonstrate that the guanine signal originated from true laser ablation (as opposed to, for example, merely heating of the source region with the laser), we unblocked and blocked the ablation laser, at 2000 shot intervals, and subtracted any background signal.] The most prominent peak in the mass spectrum ($m = 151$ amu) originates from the guanine monomer, with 3000 counts per 10 000 laser shots. This is a respectable signal for the purposes of TRPES. Experiments are currently underway in our laboratory to use fs time-resolved two-color TRPES to study the intramolecular dynamics of the isolated DNA bases. We note that cluster formation of up to five guanine molecules is also observed under the above conditions, which is an indication of cold expansion. This suggests the possibility of using such a source for studying the spectroscopy and dynamics of solvated biomolecules, DNA base

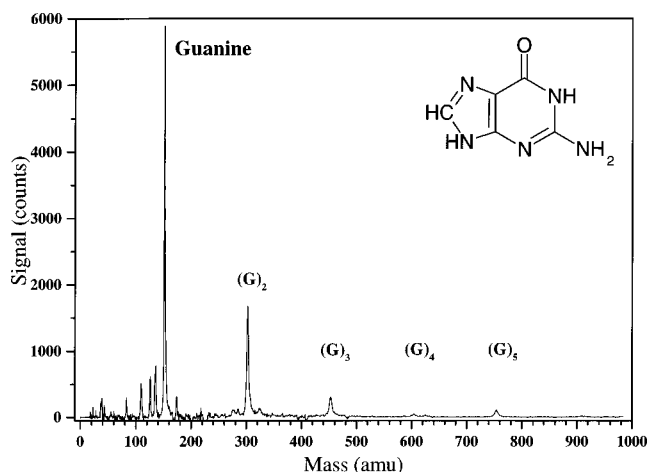


FIG. 5. Typical mass spectrum of kHz rate laser ablated guanine monomer and molecular clusters, resonantly ionized at 277 nm using 150 fs laser pulses. The count rate was 0.3 counts per laser shot (i.e., 300 counts per second), a respectable signal for many purposes. Peaks marked by an asterisk correspond to loss of the NH_2 group ($m=135$ amu) and loss of N_2CH_2 ($m=109$ amu) from the guanine monomer. For details, see the text.

pairs, etc. Fragmentation of guanine during the photoionization process⁴⁴ leads to the appearance of relatively small daughter peaks below $m=151$ amu ($m=135$ and 109 amu corresponding to NH_2 and N_2CH_2 loss, respectively). As always, the ratio of parent to fragmentation signal depends on laser energy, as does the absolute signal magnitude.

ACKNOWLEDGMENTS

The authors are grateful for the expert technical assistance of J. P. Parsons. One of the authors (S.U.) acknowledges support from a Feodor–Lynen fellowship (Alexander von Humboldt Foundation). The authors thank Professor Rainer Weinkauff for stimulating discussions.

¹See, for example, S. Backus, C. G. Durfee III, M. M. Murnane, and H. C. Kapteyn, *Rev. Sci. Instrum.* **69**, 1207 (1998).

²M. B. Knickelbein, *Philos. Mag. B* **79**, 1379 (1999).

³C. C. Hayden and A. Stolow, in *Advanced Series in Physical Chemistry*, edited by C. Y. Ng (World Scientific, Singapore, 2000), Vol. 10.

⁴D. M. Neumark, *Annu. Rev. Phys. Chem.* **52**, 255 (2001).

⁵T. Seideman, *Annu. Rev. Phys. Chem.* **53**, 41 (2002).

⁶A. Stolow, *Annu. Rev. Phys. Chem.* **54**, 89 (2003).

⁷A. Stolow, *Int. Rev. Phys. Chem.* **22**, 377 (2003).

⁸I. Fischer, M. J. J. Vrakking, D. M. Villeneuve, and A. Stolow, *Chem. Phys.* **207**, 331 (1996); A. Zavriyev, I. Fischer, D. M. Villeneuve, and A. Stolow, *Chem. Phys. Lett.* **234**, 281 (1995).

⁹T. Baer, *Int. J. Mass. Spectrom.* **200**, 443 (2000).

¹⁰V. Stert, W. Radloff, C. P. Schulz, and I. V. Hertel, *Eur. Phys. J. D* **5**, 97 (1999).

¹¹R. E. Continetti and C. C. Hayden, in *Advanced Series in Physical Chemistry: Modern Trends in Chemical Reaction Dynamics*, edited by C. Y. Ng (in press).

¹²R. E. Continetti, *Annu. Rev. Phys. Chem.* **52**, 165 (2001).

¹³M. Takahashi, J. P. Cave, and J. H. D. Eland, *Rev. Sci. Instrum.* **71**, 1337 (2000).

¹⁴P. Downie and I. Powis, *Phys. Rev. Lett.* **82**, 2864 (1999).

¹⁵S. Fredrigo, T. L. Haslett, and M. Moskovits, *J. Am. Chem. Soc.* **118**, 5083 (1996).

¹⁶D. B. Geohegan, *Laser Ablation of Electronic Materials: Basic Mechanisms and Applications*, edited by E. Fogarassy and S. Lazare (North-Holland, Amsterdam, 1992), p. 73.

¹⁷R. Kelly and A. Miotello, *Appl. Phys. B: Photophys. Laser Chem.* **57**, 145 (1993); R. Kelly, A. Miotello, B. Braren, A. Gupta, and K. Casey, *Nucl. Instrum. Methods Phys. Res. B* **65**, 187 (1992).

¹⁸D. Sibold and H. M. Urbassek, *Phys. Fluids A* **165** (1992).

¹⁹J. W. Elam and D. H. Levy, *J. Phys. Chem. B* **102**, 8113 (1998).

²⁰R. J. Levis, *Annu. Rev. Phys. Chem.* **45**, 483 (1994).

²¹R. N. Zare and R. Zenobi, *Advances in Multi-Photon Processes and Spectroscopy*, edited by S. H. Lin (World Scientific, River Edge, NJ, 1991), Vol. 7, pp. 1–168.

²²L. V. Zhigilei, E. Leveugle, B. J. Garisson, Y. G. Yingling, and M. I. Zeifman, *Chem. Rev. (Washington, D.C.)* **103**, 321 (2003).

²³J. E. Bernard and A. J. Alcock, *Opt. Lett.* **19**, 1861 (1994).

²⁴R. Campargue, *J. Phys. Chem.* **88**, 4466 (1984).

²⁵J. B. Fenn and J. Deckers, *Rarefield Gas Dynamics, 3rd Symposium*, edited by J. A. Laurmann (Academic, New York, 1963), Vol. 1.

²⁶J. B. Anderson, in *Molecular Beams and Low Density Gas Dynamics*, edited by P. P. Wegener (Dekker, New York, 1974).

²⁷M. E. Geusic, M. D. Morse, S. C. O'Brien, and R. E. Smalley, *Rev. Sci. Instrum.* **56**, 2123 (1985); M. D. Morse, M. E. Geusic, J. R. Heath, and R. E. Smalley, *J. Chem. Phys.* **83**, 2293 (1985).

²⁸S. Lochbrunner, J. J. Larsen, J. P. Schaffer, M. Schmitt, T. Schultz, J. G. Underwood, and A. Stolow, *J. Electron Spectrosc. Relat. Phenom.* **112**, 183 (2000).

²⁹See, for example, A. Assion, T. Baumert, M. Bergt, T. Brixner, B. Keifer, V. Seyfried, M. Strehle, and G. Gerber, *Science* **282**, 919 (1998).

³⁰See, for example, C. Spielmann, H. Burnett, R. Sartania, R. Koppitsch, M. Chnurrer, C. Kan, M. Lenzner, P. Wobruschek, and F. Krausz, *Science* **278**, 661 (1997).

³¹See, for example, *Laser Ablation, Proceedings of the 5th International Conference*, edited by J. S. Horwitz, H. U. Krebs, and K. Murakami (Springer, New York, 1999).

³²See, for example, B. Walker, B. Sheehy, L. F. di Mauro, P. Agostini, K. J. Schaffer, and K. C. Kulander, *Phys. Rev. Lett.* **73**, 1227 (1994).

³³M. Lezius, V. Blanchet, D. M. Rayner, D. M. Villeneuve, A. Stolow, and M. Yu. Ivanov, *Phys. Rev. Lett.* **86**, 51 (2001); M. Lezius, V. Blanchet, M. Yu. Ivanov, and A. Stolow, *J. Chem. Phys.* **117**, 1575 (2002).

³⁴S. M. Hankin, D. M. Villeneuve, P. B. Corkum, and D. M. Rayner, *Phys. Rev. Lett.* **84**, 5082 (2000).

³⁵M. Smits, C. A. de Lange, D. M. Rayner, and A. Stolow (private communication).

³⁶*Handbook of Chemistry and Physics*, 82nd ed., edited by D. R. Lide (Chemical Rubber, Boca Raton, FL, 2001).

³⁷M. A. Posthumus, P. G. Kistemaker, H. L. C. Meuzelaar, and M. C. Ten Noever de Brauw, *Anal. Chem.* **50**, 985 (1978).

³⁸G. Meijer, M. S. De Vries, H. E. Hunziker, and H. R. Wendt, *Appl. Phys. B: Photophys. Laser Chem.* **51**, 395 (1990).

³⁹A. H. Zewail, *Femtochemistry: Ultrafast Dynamics of the Chemical Bond* (World Scientific, Singapore, 1994).

⁴⁰A. H. Zewail, *J. Phys. Chem. A* **104**, 5660 (2000).

⁴¹J. Jortner, *Faraday Discuss.* **108**, 1 (1997).

⁴²V. Blanchet, M. Z. Zgierski, T. Seideman, and A. Stolow, *Nature (London)* **401**, 52 (1999); V. Blanchet, M. Z. Zgierski, and A. Stolow, *J. Chem. Phys.* **114**, 1194 (2001); M. Schmitt, S. Lochbrunner, J. P. Schaffer, J. J. Larsen, M. Z. Zgierski, and A. Stolow, *ibid.* **114**, 1206 (2001).

⁴³F. Piuze, I. Dimicoli, M. Mons, B. Tardivel, and Q. Zhao, *Chem. Phys. Lett.* **320**, 282 (2000).

⁴⁴R. Weinkauff, P. Aicher, G. Wesley, J. Grotemeyer, and E. W. Schlag, *J. Phys. Chem.* **98**, 8381 (1994).